JACS
JOURNAL OF THE AMERICAN CHEMICAL SOCIETY
Article
pubs.acs.org/JACS

Optically Active, Amphiphilic Poly(*meta*-phenylene ethynylene)s: Synthesis, Hydrogen-Bonding Enforced Helix Stability, and Direct AFM Observation of Their Helical Structures

Motonori Banno,[†] Tomoko Yamaguchi,[†] Kanji Nagai,[†,§] Christian Kaiser,[‡] Stefan Hecht,*[,‡] and Eiji Yashima*[,†]

[†]Department of Molecular Design and Engineering, Graduate School of Engineering, Nagoya University, Chikusa-ku, Nagoya, 464-8603, Japan

[‡]Department of Chemistry, Humboldt-Universität zu Berlin, Brook-Taylor-Strasse 2, 12489 Berlin, Germany

Supporting Information

ABSTRACT: Optically active, amphiphilic poly(*meta*-phenylene ethynylene)s (**PPEa**) bearing L- or D-alanine-derived oligo(ethylene glycol) side chains connected to the backbone via amide linkages were prepared by microwave-assisted polycondensation. **PPEa**'s exhibited an intense Cotton effect in the π-conjugated main-chain chromophore regions in various polar and nonpolar organic solvents due to a predominantly one-handed helical conformation stabilized by an intramolecular hydrogen-bonding network between the amide groups of the pendants. The stable helical structure was retained in the bulk and led to supramolecular column formation from stacked helices in oriented polymer films as evidenced by X-ray diffraction. Atomic force microscopy was used to directly visualize the helical structures of the polymers in two-dimensional crystalline layers with molecular resolution, and, for the first time, their absolute helical senses could unambiguously be determined.

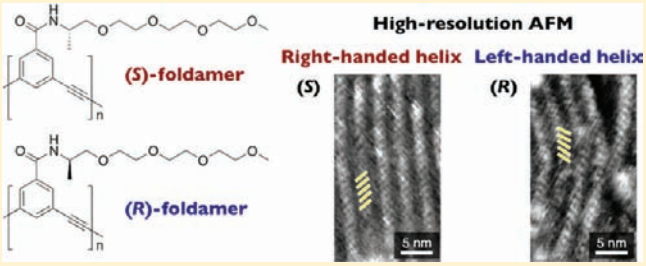

INTRODUCTION

The design and synthesis of artificial helical polymers[1] and oligomers (foldamers)[2] with a controlled helix-sense has attracted significant interest in the past two decades because of their potential applications as chiral materials for asymmetric synthesis, separation of enantiomers, and also as chiral building blocks for self-assembled nanomaterials and devices.[1c,q,r,t,3] The elucidation of their helical structures, in particular their handedness (right- or left-handed helix),[4] is quite important not only to understand the mechanism of their folding processes, but also to develop novel helical polymers and foldamers with specific functions. In contrast to proteins,[5] oligonucleotides,[6] and synthetic uniform oligomers[7] whose helical structures were unambiguously determined by their single-crystal X-ray crystallographic analyses, the exact helical structures of most of helical polymers prepared to date and some foldamers remain unknown[4] mainly due to the difficulty in obtaining crystals suitable for X-ray analysis. We now report the synthesis and chiroptical properties of a pair of novel amphiphilic poly(*meta*-phenylene ethynylene)s, carrying L- and D-alanine-derived chiral side chains and reminiscent of a foldamer-based helical polymer, and the direct observation of their helical structures by high-resolution atomic force microscopy (AFM).

meta-Linked phenylene ethynylene is one of the most popular structural motifs for foldamers developed by Moore and co-workers in 1997,[8] who prepared a series of amphiphilic oligo(*m*-phenylene ethynylene)s bearing chiral and achiral polar side chains (for example, **OPEe** and **OPEe-Me**, Chart 1) and discovered a strong tendency to fold into a helical conformation in polar solvents, such as acetonitrile and polar organic solvents driven by noncovalent, solvophobic interactions.[8] A preferred-handed helicity can be biased by diastereoselective inclusion complexation with chiral guests[9] or chiral substituents attached either in the side chains[10] or at the termini,[11] thus exhibiting an optical activity as evidenced by an appearance of strong bisignated circular dichroism (CD) signals.

After discovery of this foldamer motif, a variety of helical polymers and oligomers consisting of *m*-phenylene ethynylene or its analogous units have been prepared aiming at further developments of functional foldamers being applicable to the fields of chiral and biological materials science,[12−14] and their helical structures in solution and in the solid state have extensively been investigated by Moore and others using NMR,[8,15c] absorption,[8,15a,c] fluorescence,[8,15] CD,[9−11] and ESR[16] spectroscopies, X-ray diffraction (XRD),[17] X-ray scattering,[18] and electron microscopic[17c] methods. Molecular dynamics simulation studies on the folding processes were also

Received: April 3, 2012
Published: April 27, 2012

   dx.doi.org/10.1021/ja303204m | *J. Am. Chem. Soc.* 2012, 134, 8718−8728

Chart 1. Structures of Oligo- and Poly(*m*-phenylene ethynylene)s

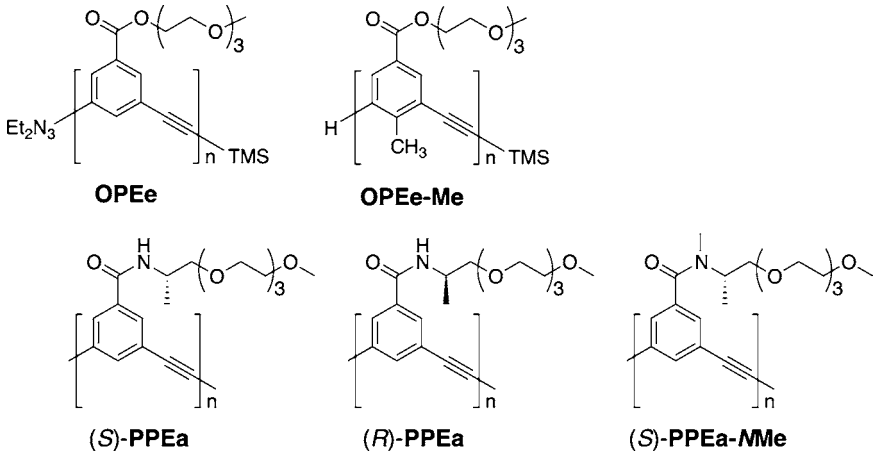

Scheme 1. Synthesis of (*S*)-PPEa and (*R*)-PPEa

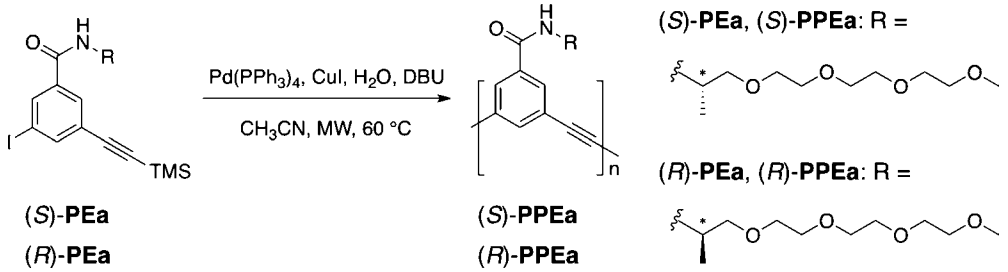

Table 1. Polymerization Results of (*S*)-PEa and (*R*)-PEa in Acetonitrile at 60 °C[a]

polymer	yield (%)[b]	$M_n \times 10^{-4}$[c]	M_w/M_n[c]	$[\alpha]^{20}_D$[d]	$\Delta\varepsilon_{first}$[e] ($M^{-1}$ cm^{-1})	$\Delta\varepsilon_{second}$[e] ($M^{-1}$ cm^{-1})
(*S*)-**PPEa**	58	10.4	3.12	+967	+113	−110
(*R*)-**PPEa**	50	10.8	2.70	−992	−118	+109

[a]Polymerized under microwave heating. [b]Isolated yield after precipitation into Et_2O and short silica column chromatography in CH_2Cl_2. [c]Determined by SEC (polystyrene standards) using a UV−visible detector with THF containing TBAB (0.1 wt %) as the eluent. [d]Measured in $CHCl_3$. [e]The first ($\Delta\varepsilon_{first}$) and second ($\Delta\varepsilon_{second}$) Cotton effects measured in $CHCl_3$.

reported.[19] A helix formation with a preferable helical sense of oligo(*m*-phenylene ethynylene) foldamers was evidenced by the appearance of CD signals,[9−11] and the helical structures including helical pitch were postulated by XRD measurements.[17b] Nevertheless, the absolute helical sense (right- or left-handed helix) of the oligo- and poly(*m*-phenylene ethynylene) foldamers with optical activity still remains unknown because of difficulty in obtaining optically active crystalline samples.

The direct observation of helical polymers by scanning probe microscopy is one of the most promising methods for providing convincing evidence of their helical structures including the helical pitch, handedness, and excess of helical handedness, but the visualization of helical structures is still challenging, and their real images of right- and left-handed helical structures by microscopy remain difficult to observe.[20]

Recently, we found that the rigid rodlike helical poly(phenylacetylene)s[21] and poly(phenyl isocyanide)s[22] bearing L- or D-alanine pendants with a long alkyl chain self-assembled to form two-dimensional (2D) crystals with regular helix-bundle structures on highly oriented pyrolytic graphite (HOPG) upon exposure to organic solvent vapors such as benzene. High-resolution AFM revealed their helical conformations in the 2D crystals and enabled us to determine the molecular length and packing, helical pitch, and handedness as well. This method has been proved to be versatile to observe helical structures of other helical polymers that involve a dynamically racemic helical poly(phenylacetylene) carrying achiral pendants,[21c] a supramolecular helical stereocomplex composed of isotactic- and syndiotactic poly(methyl methacrylate)s,[23] and a double-stranded helical polymer.[24]

In this study, we synthesized novel optically active, amphiphilic poly(*m*-phenylene ethynylene)s and investigated their preferred-handed helical structures in solution and in the solid state by absorption, CD, and IR spectroscopies as well as XRD and AFM observations. The polar chiral oligo(ethylene glycol) side chains are readily derived from either L- or D-alanine and are linked to the aromatic backbone via an amide linkage ((*S*)- or (*R*)-**PPEa**), thereby replacing the ester linkage of Moore's foldamers with an amide one (Chart 1). Because of these amide residues, the helical structures of (*S*)- and (*R*)-**PPEa** were anticipated to be stabilized by intramolecular hydrogen bonds, and the polymer backbones should therefore be more rigid than those of Moore's ester counterparts. This hydrogen-bonding intrastrand stabilization should facilitate supramolecular organization in the bulk and in particular formation of 2D crystals on a substrate while maintaining the polymers' helical conformations and indeed, for the first time, enabled us to observe hollow helical structures in oriented

dx.doi.org/10.1021/ja303204m | J. Am. Chem. Soc. 2012, 134, 8718−8728

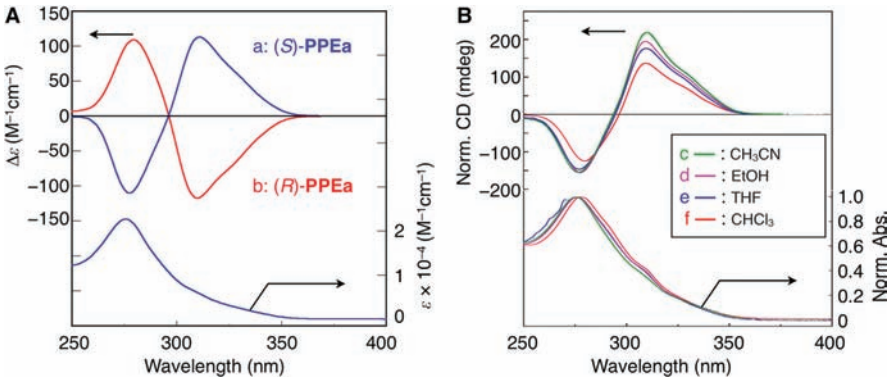

Figure 1. (A) CD and absorption spectra of (*S*)-**PPEa** (a) and (*R*)-**PPEa** (b) in $CHCl_3$ (0.5 mM) at ca. 25 °C. (B) Normalized CD and absorption spectra of (*S*)-**PPEa** in acetonitrile (c), ethanol (d), THF (e), and $CHCl_3$ (f) at ca. 25 °C. The spectra were normalized on the basis of the absorption maxima.

polymer films by XRD and to determine the absolute helical handedness of the poly(*m*-phenylene ethynylene)s by high-resolution AFM.

RESULTS AND DISCUSSION

Synthesis and Polymerization of Optically Active *m*-Phenylene Ethynylenes. The optically active monomers, *m*-trimethylsilylethynyl iodobenzenes bearing an L- or D-alanine residue with a tri(ethylene glycol) as the pendant through an amide linkage ((*S*)- or (*R*)-**PEa**, respectively), were synthesized as outlined in Schemes S1−S4, and these were polymerized according to the previously reported method using the microwave-assisted polycondensation[25] in acetonitrile at 60 °C (Scheme 1). The polymerization results are summarized in Table 1. The polymerization of (*S*)-**PEa** and (*R*)-**PEa** homogeneously proceeded, yielding high molecular weight polymers as an orange-brown solid in moderate yield (58% and 50%, respectively). The number-average molecular weight (M_n) and its distribution (M_w/M_n) were estimated to be 10.4×10^4 and 3.12 for (*S*)-**PPEa** as well as 10.8×10^4 and 2.70 for (*R*)-**PPEa**, as determined by size exclusion chromatography (SEC) with polystyrene standards using tetrahydrofuran (THF) containing 0.1 wt % tetra-*n*-butylammonium bromide (TBAB) as the eluent.

Chiroptical Properties in Dilute Solution. Moore and co-workers previously reported that oligo(*m*-phenylene ethynylene)s bearing electron-withdrawing ester residues with polar tri(ethylene glycol) chains as the pendants (**OPEe**, Chart 1) solvophobically fold into helical conformations in polar solvents, such as acetonitrile and aqueous organic solutions.[8] This strong tendency of helical folding is attributed to the intramolecular $\pi-\pi$ stacking between nonadjacent electron-poor phenylene ethynylene residues in conjunction with the favorable interactions between the polar side chains and the polar solvent, while the nonpolar folded backbone is hidden from the polar solvent. On the contrary, in less polar "good" solvents for both backbone and side chains, such as $CHCl_3$, the oligomers adopt a random-coil conformation. These conformational states are also dependent on the chain-length[8c,15a] and temperature[8a,15b] as well as solvent polarities.[11c]

On the basis of these precedents, we first investigated the solvent effects on the chiroptical properties of **PPEa**s in a dilute solution by measuring the absorption and CD spectra of (*S*)-**PPEa** and (*R*)-**PPEa** in various solvents. Figure 1A shows the typical CD and absorption spectra of (*S*)-**PPEa** and (*R*)-**PPEa** in $CHCl_3$. In sharp contrast to the ester-bound oligo(*m*-phenylene ethynylene)s (**OPEe**) prepared by the group of Moore, the polymers exhibited intense, bisignated Cotton effects in the π-conjugated phenylene ethynylene chromophore regions (250−365 nm) that are mirror images of each other. The monomers showed negligible CD at wavelengths greater than 275 nm. These results indicate that (*S*)-**PPEa** and (*R*)-**PPEa** possess a preferred-handed helical conformation with an opposite helix-sense induced by the covalent-bonded chiral alanine pendants even in $CHCl_3$, in which the ester-bound **OPEe** exhibited no CD at all in the presence of chiral guests, independent of the chain length.[9] In $CHCl_3$, the helical conformation of **PPEa**'s is most likely stabilized by intramolecular hydrogen bonds between the nonadjacent amide residues, so that the CD and absorption spectra hardly changed in $CHCl_3$ even at 55 °C. The IR spectra of **PPEa** measured in $CHCl_3$ supported the intramolecular hydrogen-bond networks; sharp signals assigned to the amide NH and carbonyl stretching (amide I) bands appeared at approximately 3274 and 1633 cm^{-1}, respectively,[26] while those of the corresponding monomer shifted to higher wavenumbers at 3439 and 1655 cm^{-1}, respectively (Table S1 and Figure S1).

(*S*)-**PPEa** also displayed similar CDs in their patterns but with more intense Cotton effect intensities in polar solvents, such as acetonitrile, ethanol, and THF and their absorption maxima slightly shifted to a shorter wavelength as compared to that in $CHCl_3$ (Figure 1B), indicative of the polymer adopting an excess one-handed helical conformation in these polar solvents. The magnitude of the Cotton effects that reflects the helical sense excess of the polymer increased with an increase in the polarity of the solvents;[11c] the observed CD intensity increased in the order $CHCl_3$ < THF < ethanol < acetonitrile. In THF and ethanol, however, such hydrogen bonding would be weakened. Nevertheless, the polymer maintained its helical structure because of favorable solvophobic interactions between the polar side chains of **PPEa** and solvents, which is capable of strengthening the aromatic $\pi-\pi$ interactions, resulting in the folded helical conformation.[8]

Addition of 2,2,2-trifluoroethanol (TFE) as a hydrogen-bond competitor to a $CHCl_3$ solution of (*S*)-**PPEa** caused a significant decrease in the Cotton effects, and the CD completely disappeared in the presence of a small amount of TFE (2.5 vol %) (Figure 2). These sudden changes in the CD spectra were accompanied by a large red-shift in the absorption up to ca. 13 nm along with an appearance of a new peak at 307

dx.doi.org/10.1021/ja303204m | J. Am. Chem. Soc. 2012, 134, 8718−8728

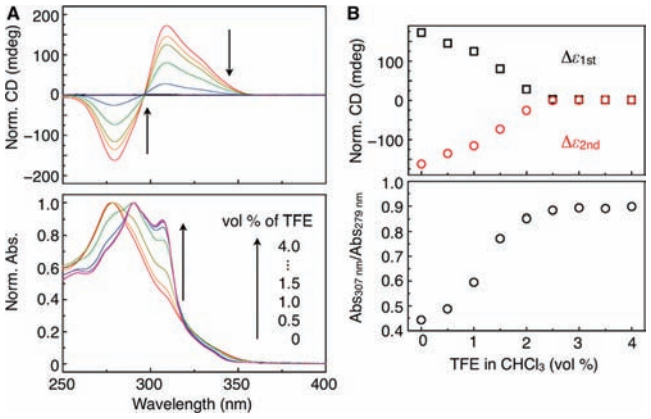

Figure 2. (A) CD (top) and absorption (bottom) spectral changes of (*S*)-**PPEa** with the increasing volume fraction of TFE in $CHCl_3$ at 25 °C. (B) Changes in the CD intensities at the first ($\Delta\varepsilon_{first}$) and second ($\Delta\varepsilon_{second}$) Cotton effects and the intensity ratio of the absorption maxima at 279 and 307 nm (Abs_{307}/Abs_{279}) versus volume % of TFE in $CHCl_3$. The spectra were normalized on the basis of the absorption maxima.

nm (Figure 2A) derived from a transoid conformation of the *m*-phenylene ethylene units, leading to a random coil induced by TFE,[8,15a] which hampered the intramolecular hydrogen-bond networks of **PPEa** chains. This interpretation is supported by the fact that the NH and amide I bands of **PPEa** in a $CHCl_3$–TFE mixture (100/5 (v/v)) significantly shifted to higher wavenumbers accompanied by band broadening and/or splitting in its IR spectrum (Table S1 and Figure S1).

An intriguing phenomenon was observed when the CD spectra of (*S*)-**PPEa** in $CHCl_3$ solutions containing minor amounts of TFE were investigated as a function of temperature. Unexpectedly, partial denaturation caused by small amounts (2 vol %) of TFE in $CHCl_3$ at room temperature was not completed by additional heating of the sample, but, on the contrary, refolding was observed at elevated temperatures (Figure 3A). The folding transition temperatures are highly sensitive to the amount of TFE present, showing a strong increase with the increasing TFE content ranging from 1.0 to 2.5 vol % in $CHCl_3$ (Figure 3B). At first glance, this anomalous "inverse melting" behavior seems to contradict classical temperature-induced denaturation experiments with biopolymers, such as polypeptides/proteins or DNA, in which higher temperatures provide the enthalpy necessary to break the noncovalent interactions responsible for folding.[2b] However, in the present case, the polymer is denatured in $CHCl_3$ at low temperatures because the TFE successfully interrupts the intramolecular amide hydrogen-bonding network by forming intermolecular hydrogen bonds to the amides (as it is present in large excess as compared to the polymers' amide residues). When such a system is subsequently heated, the TFE–amide contacts are broken, and the intramolecular hydrogen-bonding network is reinstalled leading to folding that is thermodynamically driven by the release of TFE. Hence, the "inverse melting" behavior appears to be entropic in origin.

The importance of the intramolecular hydrogen-bonding network between the amide residues is perhaps most apparent when comparing the folding behavior of (*S*)-**PPEa** (vide supra) with its *N*-methylated derivative (*S*)-**PPEa-*N*Me** (Chart 1), which can readily be prepared by direct *N*-methylation using excess methyl iodide in the presence of excess sodium hydride as the base (see the Supporting Information). Almost complete *N*-methylation was clearly visible from the ^{1}H NMR spectra (Figure S2) that furthermore showed much narrower peaks, indicating the absence of π–π stacking interactions and hence an unfolded random coil conformation. Much more impressively, the absence of any CD signal as well as the occurrence of transoid absorption bands unambiguously demonstrate that (*S*)-**PPEa-*N*Me** adopts a random coil conformation, regardless of the solvent (Figure S3). Even in the folding-promoting solvent CH_3CN, (*S*)-**PPEa-*N*Me** is not folding, demonstrating the importance of the hydrogen-bonding for helix formation in (*S*)-**PPEa** and the slightly more electron-rich character of the amide-substituted *m*-phenylene ethynylene units, leading to weaker π–π stacking contacts (as compared to their ester counterparts, which fold under these conditions).[15c]

Helical Structure of PPEa. To obtain structural information of **PPEa** in the solid state, wide-angle X-ray diffraction (WAXD) measurements of oriented **PPEa** films were performed. Samples for the WAXD measurements were prepared from a concentrated $CHCl_3$ solution in a magnetic field (11.75 T overnight) by slow evaporation,[22b] and the films exhibited a birefringence as observed by polarizing optical microscopy (Figure 4G). Figure 4A–D shows the WAXD patterns of the magnetically oriented **PPEa** films, which displayed diffuse, but apparent equatorial and near-meridional reflections. The four equatorial reflections, 27.29, 15.89, 13.62, and 10.37 Å for (*S*)-**PPEa** and 27.22, 15.52, 13.64, and 10.20 Å for (*R*)-**PPEa**, can be indexed with a 2D hexagonal lattice of a = 31.51 and 31.43 Å, respectively, and the observed d-spacings are listed in Table 2. The strong meridional reflections at 3.56 Å for (*S*)-**PPEa** and 3.55 Å for (*R*)-**PPEa** most likely correspond to the spacing between the π-stacked benzene units,[27] which were in accordance with those reported for the *endo*-methyl substituted *m*-phenylene ethynylene oligomers (**OPEe-Me**, Chart 1) (Table S2). Moore and co-workers previously reported that the introduction of methyl groups into the

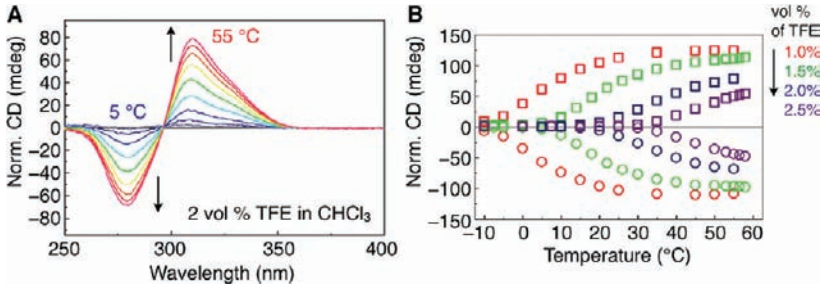

Figure 3. (A) CD spectral changes of (*S*)-**PPEa** with varying temperature (5–55 °C) in $CHCl_3$ containing 2 vol % TFE. (B) Changes in the CD intensities at the first ($\Delta\varepsilon_{first}$) and second ($\Delta\varepsilon_{second}$) Cotton effects versus temperature at varying amounts of TFE (1.0–2.5 vol %) in $CHCl_3$.

dx.doi.org/10.1021/ja303204m | *J. Am. Chem. Soc.* 2012, 134, 8718–8728

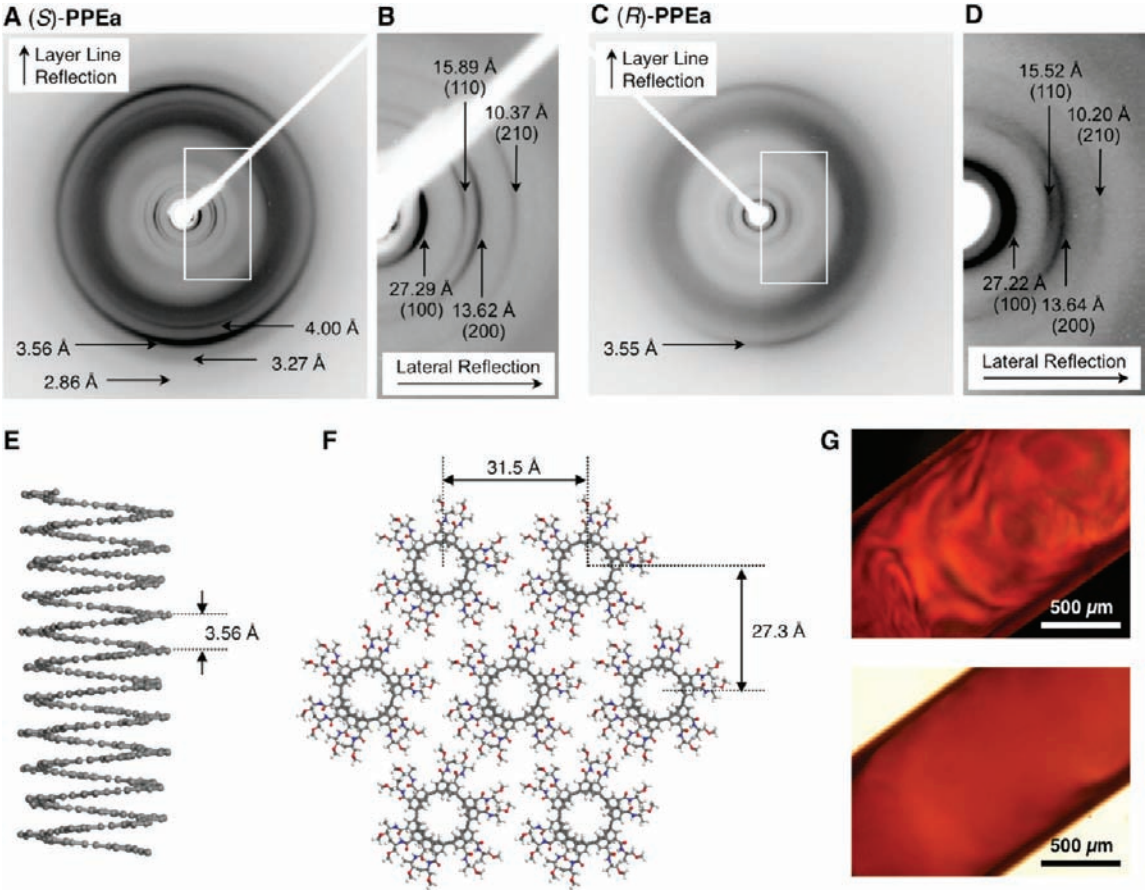

Figure 4. X-ray diffraction patterns of oriented (*S*)-**PPEa** (A) and (*R*)-**PPEa** (C) films prepared from concentrated $CHCl_3$ solutions (ca. 16 wt %). The magnified X-ray diffraction patterns corresponding to the area indicated by the white squares in (A) and (C) are shown in (B) and (D), respectively. (E) Optimized right-handed helical structure of (*S*)-**PPEa** on the basis of XRD structural analyses followed by molecular mechanics calculations (see the Supporting Information). The main-chain carbon atoms are shown using the ball and stick model, and the pendant tri(ethylene glycol) chains are omitted for clarity. The helical pitch (3.56 Å) corresponding to $\pi-\pi$ stacking is also shown. (F) Schematic illustration of a possible hexagonal packing of (*S*)-**PPEa**. (G) Polarized (top) and nonpolarized (bottom) optical micrographs of an (*R*)-**PPEa** film.

Table 2. X-ray Diffraction Data of Oriented (*S*)- and (*R*)-PPEa Films

(*S*)-PPEa				(*R*)-PPEa			
d_{obs}/Å[a]	d_{cal}/Å[b]	*hkl*	I_{obs}[c]	d_{obs}/Å[a]	d_{cal}/Å[b]	*hkl*	I_{obs}[c]
27.29	27.29	100	vs	27.22	27.22	100	vs
15.89	15.76	110	w	15.52	15.72	110	m
13.62	13.65	200	s	13.64	13.61	200	s
10.37	10.31	210	m	10.20	10.29	210	w

[a]Spacings observed in X-ray diffraction patterns of (*S*)- and (*R*)-**PPEa** oriented films. [b]Spacings calculated and indexed on the basis of hexagonal unit cells with parameters a = 31.51 Å for (*S*)-**PPEa** and 31.43 Å for (*R*)-**PPEa**. [c]Observed intensities: vs = very strong, s = strong, m = medium, and w = weak.

endo-positions of *m*-phenylene ethylene oligomers (**OPEe-Me**) resulted in the formation of helical nanotubules with a similar hexagonal arrangement in the solid state, whereas the corresponding *m*-phenylene ethylene oligomers packed into a lamellar arrangement, presumably to avoid formation of hollow interior channels.[17b] Comparison of helical structures of **PPEa** with those of Moore's oligomers **OPEe-Me** revealed that the X-ray diffraction patterns are very similar to one another. Although the hexagonal lattice of **PPEa** (31–32 Å) appears to be slightly larger than those of **OPEe-Me** (30 Å),[17b] it seems reasonable by taking into account the longer side chain of **PPEa** as compared to **OPEe-Me**. Figure 4E and F illustrates the molecular structures of the right-handed helical (*S*)-**PPEa** model (60-mer) and its hexagonal packing, respectively, estimated on the basis of the XRD data. It should be emphasized that **PPEa**'s carrying no methyl groups at the *endo*-positions fold into a helical conformation in a variety of polar and nonpolar solvents and further self-assemble into columnar nanotubules as stabilized by the intramolecular hydrogen-bonding networks. In strong contrast, the corresponding ester-linked **OPEe**'s that form a helical conformation in specific polar solvents cannot maintain their helical structure in the bulk and adopt a zigzag conformation to pack into a lamellar arrangement.[17]

Although *m*-phenylene ethynylene oligomers have been considered to have a ~6 units per turn[16] helical conformation in polar solvents such as acetonitrile and in the solid state for **OPEe-Me**, their exact helical structures, in particular, the helical sense, have not yet been elucidated unambiguously, most likely because of the difficulty in obtaining a single-crystal suitable for X-ray crystallographic analysis.[17b] To gain further insight, theory employing molecular mechanics simulations was used for postulating the helical sense of foldamer-based helical oligomers and polymers, such as *m*-phenylene ethynylene oligomers containing an optically active helicene unit,[11d] *m*-

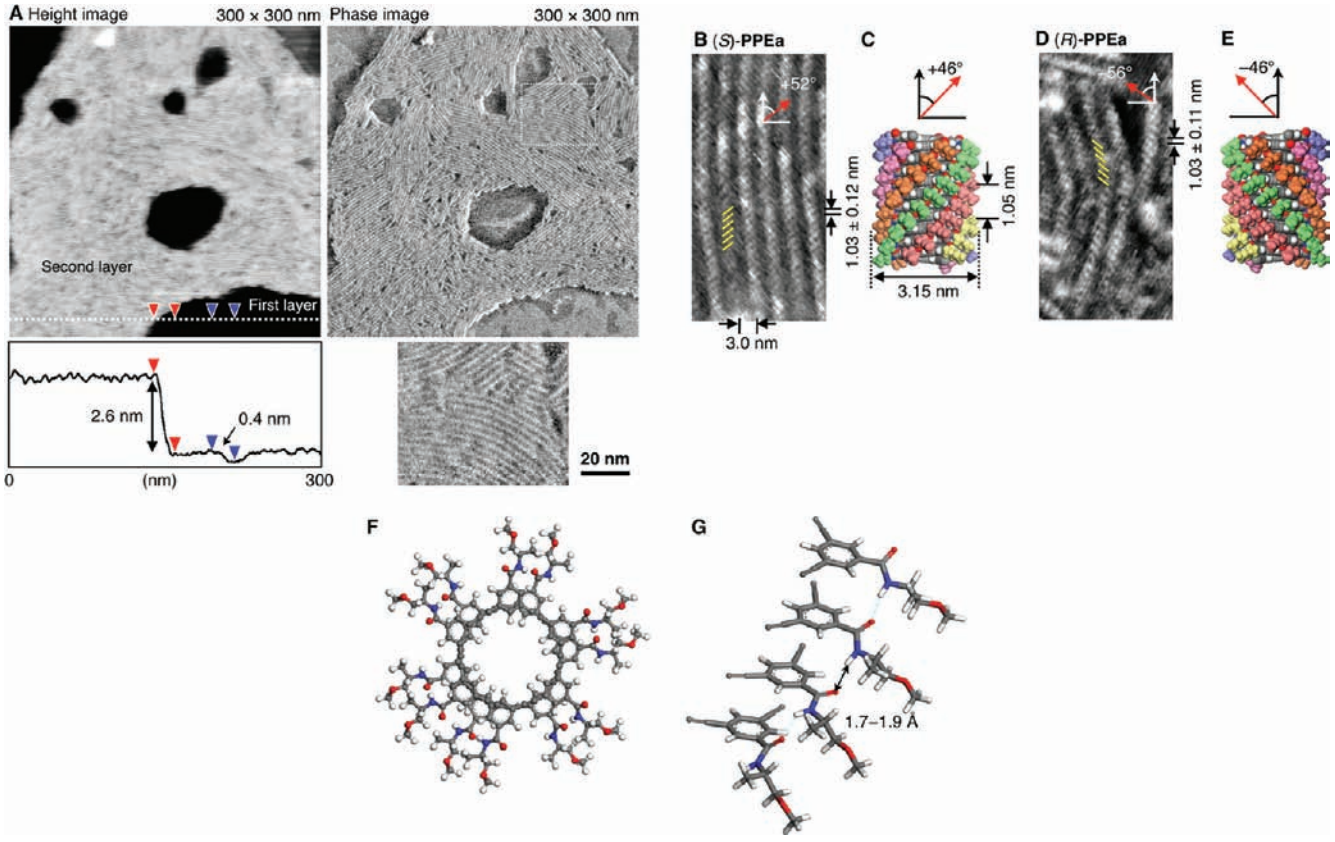

Figure 5. (A) AFM height (left) and phase (right) images of (*S*)-**PPEa** on HOPG (scale = 300 × 300 nm) prepared by casting a dilute $CHCl_3$ solution (0.02 mg/mL). The cross-section profile denoted by the white dashed line and the zoomed image corresponding to the area indicated by the square are also shown. (B,D) High-resolution AFM phase images of (*S*)-**PPEa** (B) and (*R*)-**PPEa** (D) on HOPG (scale = 40 × 20 nm). Schematic representations of the right-handed helical (*S*)-**PPEa** and left-handed helical (*R*)-**PPEa** structures with periodic oblique stripes (yellow lines), which denote a one-handed helical array of the pendants, are also shown. For wider AFM images of 2D self-assembled (*S*)-**PPEa** and (*R*)-**PPEa**, see Figures S6 and S7, respectively. (C,E) Optimized helical structures of (*S*)-**PPEa** (C, 60-mer) and (*R*)-**PPEa** (E, 60-mer) calculated on the basis of XRD structural analyses followed by molecular mechanics calculations (see the Supporting Information). Each structure is represented by space-filling models, and six sets of hydrogen-bonded helical arrays (*n* and *n* + 6) of the pendants are shown in different colors for clarity. (F,G) The detailed helical structures of (*S*)-**PPEa** (12-mer) taken from (C) are also shown by a ball and stick model in (F) (top view) and (G) (side view). In these models, the long oligo(ethylene glycol) side groups were replaced by terminal methyl groups for clarity.

ethynylpyridine oligomers bearing saccharide moieties as the terminal,[13d] and azobenzene-bound poly(*m*-phenylene ethynylene) containing D-amino acid residues.[12j] Optically active poly(*m*-phenylene ethynylene-*alt*-*p*-phenylene ethynylene)s bearing chiral pendants were also suggested to adopt a left[14b]- or right[14c,d]-handed helix in solution judging from the Cotton effect patterns in their CD spectra. However, these computational methods certainly involve a significant uncertainty, and hence an experimental approach for reliable structure elucidation is highly desirable.

Recently, we developed a facile method to directly observe the helical structures of several synthetic helical polymers including poly(phenylacetylene)s bearing L- or D-alanine residues with a long alkyl chain as the pendants.[21] Flat poly(phenylacetylene) monolayers were first formed epitaxially on the basal plane of the graphite, on which helical poly(phenylacetylene) further self-assembled into chiral 2D helix-bundled crystals upon exposure to organic solvent vapors.[21a] The surface of the 2D crystals was extremely smooth and flat, which enabled us to observe high-resolution AFM images and to determine the molecular packing, helical pitch, and handedness when combined with XRD analysis. Hence, we applied this procedure to visualize the helical structures of (*S*)- and (*R*)-**PPEa**'s on HOPG.

Figure 5A shows a typical AFM image of (*S*)-**PPEa** deposited on HOPG from a dilute $CHCl_3$ solution (0.02 mg/mL) under a nitrogen atmosphere[28] at ambient temperature. (*S*)-**PPEa** self-assembled into well-defined 2D helix-bundles with a constant height of 2.6 nm, indicating the polymer maintains its folded structure on HOPG. Careful observation of the AFM image together with an additional experiment (Figure S4)[29] suggests that a regular monolayer composed of nonhelical (*S*)-**PPEa** chains with a planar conformation (an average height of 0.4 nm (first layer); see Figures 5A and S4) was first formed on the graphite substrate, on which the 2D helix-bundled (*S*)-**PPEa** chains with controlled helicity and lateral packing were generated, as observed for helical poly(phenylacetylene)s.[21a] The bundle structures were clearly resolved into individual polymer chains packed parallel to each other with a chain-to-chain spacing of ca. 3.0 nm, which is in good agreement with that deduced from the XRD measurements (3.15 nm).

The high-resolution AFM images of (*S*)- and (*R*)-**PPEa**'s revealed a number of periodic oblique stripes (yellow lines in Figure 5B and D), probably originating from a one-handed helical array of the pendants that were tilted clockwise or

dx.doi.org/10.1021/ja303204m | *J. Am. Chem. Soc.* 2012, 134, 8718−8728

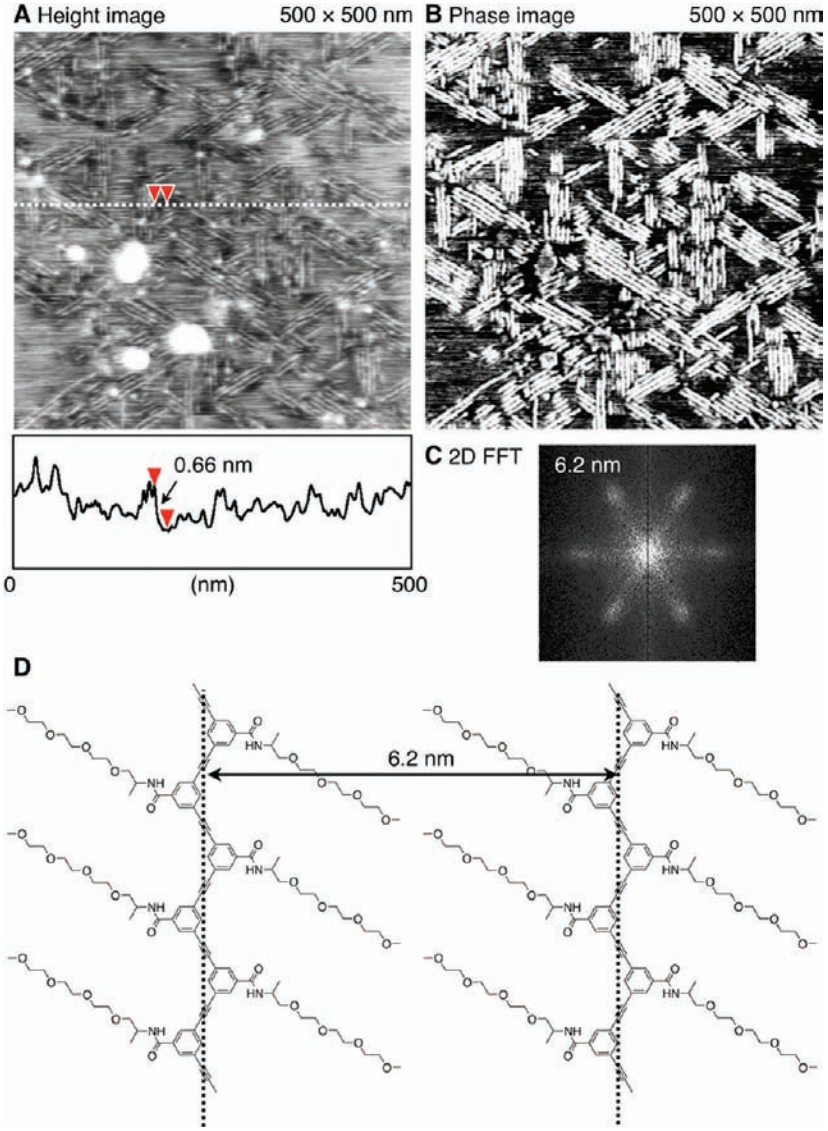

Figure 6. AFM height (A) and phase (B) images of (*S*)-**PPEa** prepared by casting a dilute $CHCl_3$/TFE solution (96/4, v/v, 0.02 mg/mL) on HOPG (scale = 500 × 500 nm). The cross-section profile denoted by the white dashed line in (A) is also shown. (C) Typical 2D fast Fourier transform of the phase image in (B) indicating the periodicity of 6.2 nm. (D) Schematic representation of the **PPEa** chains lying flat on the substrate with a planar conformation aligned parallel to the graphite lattice.

counterclockwise at +52° and −56° with respect to the main-chain axis for (*S*)-**PPEa** and (*R*)-**PPEa**, respectively. This remarkable 2D mirror-image relationship suggests that (*S*)-**PPEa** and (*R*)-**PPEa** have enantiomeric right- and left-handed helical structures with a helical pitch of 1.03 ± 0.12 and 1.03 ± 0.11, respectively, as estimated from the average distance between each stripe. The helical pitch obtained from the AFM images is almost identical to the helical pitches of the pendant helical arrangements as estimated from the molecular model constructed on the basis of the XRD structural analyses followed by molecular mechanics calculations (Figure 5C and E). The detailed structures (12-mer) taken from Figure 5C are also shown in Figure 5F and G (see also the Supporting Information). The polymer models appear to have six sets of hydrogen-bonded helical arrays linking *n* and (*n* + 6) pendants with the one-sixth helical pitch of 1.05 nm.[30] On the basis of an evaluation of more than 300 individual polymer chains in the 2D helix-bundles, the number-average molecular length (L_n) and the length distribution (L_w/L_n) were also estimated to be 21.5 ± 12.2 nm and 1.34 for (*S*)-**PPEa** as well as 18.9 ± 8.51 nm and 1.20 for (*R*)-**PPEa**. The degree of polymerization (DP) was then calculated using the helical parameter, 5.7 units per turn (3.6 Å), to be 340 and 299 for (*S*)-**PPEa** and (*R*)-**PPEa**, respectively (Figure S5). These values correspond to M_n = 11.8 × 10^4 for (*S*)-**PPEa** and M_n = 10.4 × 10^4 for (*R*)-**PPEa**, in good agreement with the values determined by SEC (vide supra).

The effect of TFE on the self-assembled **PPEa** structure on HOPG was also investigated. Figure 6 shows the AFM image of (*S*)-**PPEa** prepared by casting a dilute $CHCl_3$ solution containing 4 vol % of TFE on HOPG. The **PPEa** molecules spontaneously self-assembled into a highly ordered monolayer as evidenced by parallel stripes with a periodicity of ca. 6.2 nm. The 2D fast Fourier transform of this monolayer showed 3-fold symmetry (Figure 6C), reflecting the crystallographic structure of the HOPG substrate. The average height of the monolayer was ca. 0.7 nm. These results indicate that the **PPEa** molecules lie flat on the substrate with a planar conformation aligned parallel to the graphite lattice, probably because of the strong

dx.doi.org/10.1021/ja303204m | *J. Am. Chem. Soc.* 2012, 134, 8718−8728

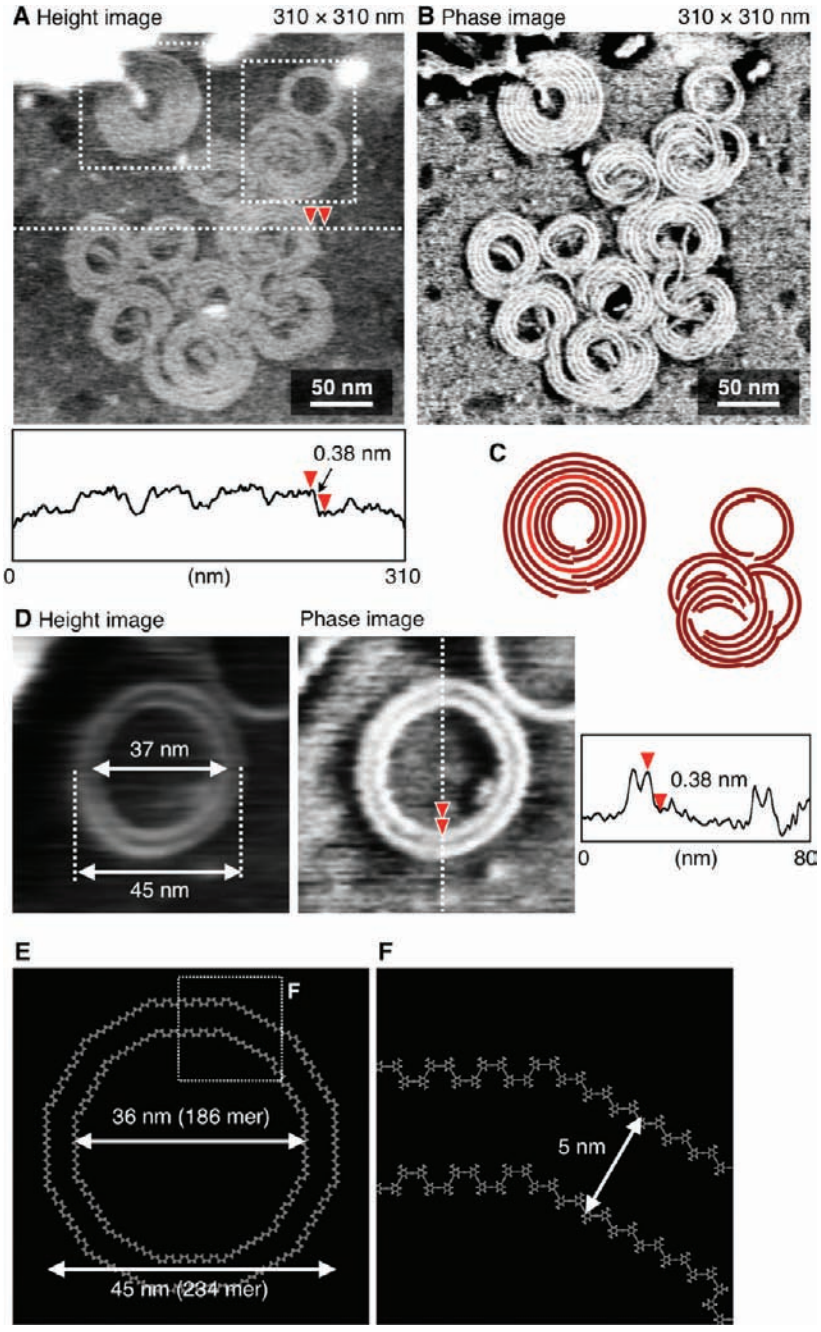

Figure 7. AFM height (A) and phase (B) images of onion-like assemblies of (*S*)-**PPEa** on HOPG (scale = 310 × 310 nm) prepared by casting a dilute $CHCl_3$ solution (0.02 mg/mL). The cross-section profile denoted by the white dashed line in (A) is also shown. (C) Schematic illustration for onion-like assemblies corresponding to the area indicated by the squares in (A). A cyclic chain is shown in red. (D) AFM height and phase images of cyclic (*S*)-**PPEa** chains and its molecular model (E,F). The cross-section height profile measured along the white dashed line is also shown in (D).

and epitaxial adsorption of the long pendant chains on HOPG (Figure 6B and D).

Interestingly, besides 2D-assembled helical **PPEa** chains (Figure 5), cyclic molecules (Figure 7D) and onion-like assembled **PPEa** chains (Figure 7A and B) with a similar height of ca. 0.4 nm were also observed during the high-resolution AFM observations when casting a dilute $CHCl_3$ solution (0.02 mg/mL) of (*S*)-**PPEa** on HOPG. Such cyclic polymers could be inevitably generated during the polycondensation reaction of the monomers, followed by the termination.[31] The onion-like assemblies seem to consist of a few cyclic polymers around which linear polymers may be assembled (Figure 7C). Figure 7D shows a double-ring assembly with a diameter of 37 and 45 nm for an inner ring and outer ring, respectively, which correspond to 186 and 234 monomer units (Figure 7E and F). The mechanism for such ring-like assembly formations is not clear at present, but may be ascribed to a template effect of the cyclic polymers that probably nucleate the assemblies of linear polymers.[32]

■ CONCLUSIONS

We have successfully synthesized optically active, amphiphilic poly(*m*-phenylene ethynylene)s carrying chiral tri(ethylene glycol) side chains derived from L- or D-alanine and attached

dx.doi.org/10.1021/ja303204m | *J. Am. Chem. Soc.* 2012, 134, 8718−8728

to the aromatic backbone via an amide linkage. In sharp contrast to the analogous ester-linked oligo(*m*-phenylene ethynylene)s, the amide-linked polymers adopt remarkably stable, excess one-handed helical conformations in a variety of polar and nonpolar solvents. The helical structure is stabilized by six sets of intramolecular hydrogen-bonding helical arrays between the pendants as characterized by absorption, CD, and FT-IR spectroscopies, as well as comparison with the corresponding *N*-methylated derivative. Because of its exceptional stability, the helix was retained even in the solid state, allowing its unprecedented structural characterization. Therefore, for the first time, the helical structures of *m*-phenylene ethynylene foldamers including the helical pitch and helical sense could unambiguously be determined by high-resolution AFM observations combined with X-ray diffraction measurements. The present study implies that previously unsolved helical structures of other helical polymers and oligomers,[1r,4] and π-stacked supramolecular helical assemblies derived from small molecules,[1j] may be determined by high-resolution AFM if 2D self-assembled helix-bundled crystals are available on substrates. From a more applied perspective, the finding that during the hierarchical supramolecular organization of our polymers their hollow helical structure is retained in the solid state offers the prospect of engineering chiral nanoporous materials, suitable for separation and sensing of (chiral) compounds and analytes, respectively.

■ ASSOCIATED CONTENT

Supporting Information

Experimental details. This material is available free of charge via the Internet at http://pubs.acs.org.

■ AUTHOR INFORMATION

Corresponding Author

sh@chemie.hu-berlin.de; yashima@apchem.nagoya-u.ac.jp

Present Address

[§]Department of Applied Chemistry, Graduate School of Engineering, Nagoya University, Chikusa-ku, Nagoya, 464−8603, Japan.

Notes

The authors declare no competing financial interest.

■ ACKNOWLEDGMENTS

This work was supported in part by a Grant-in-Aid for Scientific Research (S) from the Japan Society for the Promotion of Science (JSPS) and the Global COE Program "Elucidation and Design of Materials and Molecular Functions" of the Ministry of Education, Culture, Sports, Science, and Technology, Japan. M.B. expresses his thanks for the JSPS Research Fellowship for Young Scientists (No. 9164).

■ REFERENCES

(1) (a) Green, M. M.; Park, J.-W.; Sato, T.; Teramoto, A.; Lifson, S.; Selinger, R. L. B.; Selinger, J. V. *Angew. Chem., Int. Ed.* **1999**, *38*, 3138−3154. (b) Mayer, S.; Zentel, R. *Prog. Polym. Sci.* **2001**, *26*, 1973−2013. (c) Nakano, T.; Okamoto, Y. *Chem. Rev.* **2001**, *101*, 4013−4038. (d) Cornelissen, J. J. L. M.; Rowan, A. E.; Nolte, R. J. M.; Sommerdijk, N. A. J. M. *Chem. Rev.* **2001**, *101*, 4039−4070. (e) Fujiki, M.; Koe, J. R.; Terao, K.; Sato, T.; Teramoto, A.; Watanabe, J. *Polym. J.* **2003**, *35*, 297−344. (f) Yashima, E.; Maeda, K.; Nishimura, T. *Chem.-Eur. J.* **2004**, *10*, 42−51. (g) Lockman, J. W.; Paul, N. M.; Parquette, J. R. *Prog. Polym. Sci.* **2005**, *30*, 423−452. (h) Lam, J. W. Y.; Tang, B. Z. *Acc. Chem. Res.* **2005**, *38*, 745−754. (i) Aoki, T.; Kaneko, T.; Teraguchi, M. *Polymer* **2006**, *47*, 4867−4892. (j) Maeda, K.; Yashima, E. *Top. Curr. Chem.* **2006**, *265*, 47−88. (k) Rudick, J. G.; Percec, V. *New J. Chem.* **2007**, *31*, 1083−1096. (l) Masuda, T. *J. Polym. Sci., Part A: Polym. Chem.* **2007**, *45*, 165−180. (m) Yashima, E.; Maeda, K. *Macromolecules* **2008**, *41*, 3−12. (n) Yashima, E.; Maeda, K.; Furusho, Y. *Acc. Chem. Res.* **2008**, 1166−1180. (o) Pijper, D.; Feringa, B. L. *Soft Matter* **2008**, *4*, 1349−1372. (p) Kim, H.-J.; Lim, Y.-B.; Lee, M. *J. Polym. Sci., Part A: Polym. Chem.* **2008**, *46*, 1925−1935. (q) Liu, J.; Lam, J. W. Y.; Tang, B. Z. *Chem. Rev.* **2009**, *109*, 5799−5867. (r) Yashima, E.; Maeda, K.; Iida, H.; Furusho, Y.; Nagai, K. *Chem. Rev.* **2009**, *109*, 6102−6211. (s) Furusho, Y.; Yashima, E. *J. Polym. Sci., Part A: Polym. Chem.* **2009**, *47*, 5195−5207. (t) Schwartz, E.; Koepf, M.; Kitto, H. J.; Nolte, R. J. M.; Rowan, A. E. *Polym. Chem.* **2011**, *2*, 33−47. (u) Kennemur, J. G.; Novak, B. M. *Polymer* **2011**, *52*, 1693−1710.

(2) (a) Gellman, S. H. *Acc. Chem. Res.* **1998**, *31*, 173−180. (b) Hill, D. J.; Mio, M. J.; Prince, R. B.; Hughes, T. S.; Moore, J. S. *Chem. Rev.* **2001**, *101*, 3893−4011. (c) Seebach, D.; Beck, A. K.; Bierbaum, D. J. *Chem. Biodiversity* **2004**, *1*, 1111−1239. (d) Huc, I. *Eur. J. Org. Chem.* **2004**, 17−29. (e) *Foldamers: Structure, Properties, and Applications*; Hecht, S., Huc, I., Eds.; Wiley-VCH: Weinheim, 2007. (f) Goodman, C. M.; Choi, S.; Shandler, S.; DeGrado, W. F. *Nat. Chem. Biol.* **2007**, *3*, 252−262. (g) Li, Z.-T.; Hou, J.-L.; Li, C. *Acc. Chem. Res.* **2008**, *41*, 1343−1353. (h) Gong, B. *Acc. Chem. Res.* **2008**, *41*, 1376−1386. (i) Saraogi, I.; Hamilton, A. D. *Chem. Soc. Rev.* **2009**, *38*, 1726−1743. (j) Ni, B.-B.; Yan, Q.; Ma, Y.; Zhao, D. *Coord. Chem. Rev.* **2010**, *254*, 954−971. (k) Guichard, G.; Huc, I. *Chem. Commun.* **2011**, *47*, 5933−5941. (l) Roy, A.; Prabhakaran, P.; Baruah, P. K.; Sanjayan, G. J. *Chem. Commun.* **2011**, *47*, 11593−11611.

(3) (a) Goh, M.; Matsushita, S.; Akagi, K. *Chem. Soc. Rev.* **2010**, *39*, 2466−2476. (b) Kane-Maguire, L. A. P.; Wallace, G. G. *Chem. Soc. Rev.* **2010**, *39*, 2545−2576. (c) Ho, R.-M.; Chiang, Y.-W.; Lin, S.-C.; Chen, C.-K. *Prog. Polym. Sci.* **2011**, *36*, 376−453.

(4) Yashima, E. *Polym. J.* **2010**, *42*, 3−16.

(5) Schulz, G. E.; Schirmer, R. H. *Principles of Protein Structure*; Springer-Verlag: New York, 1979.

(6) (a) Saenger, W. *Principles of Nucleic Acid Structure*; Springer-Verlag: New York, 1984. (b) Kennard, O.; Hunter, W. N. *Angew. Chem., Int. Ed. Engl.* **1991**, *30*, 1254−1277.

(7) (a) Ute, K.; Hirose, K.; Kashimoto, H.; Nakayama, H.; Hatada, K.; Vogl, O. *Polym. J.* **1993**, *25*, 1175−1186. (b) Ito, Y.; Ohara, T.; Shima, R.; Suginome, M. *J. Am. Chem. Soc.* **1996**, *118*, 9188−9189. (c) Tanatani, A.; Yokoyama, A.; Azumaya, I.; Takakura, Y.; Mitsui, C.; Shiro, M.; Uchiyama, M.; Muranaka, A.; Kobayashi, N.; Yokozawa, T. *J. Am. Chem. Soc.* **2005**, *127*, 8553−8561. (d) Dolain, C.; Jiang, H.; Léger, J.-M.; Guionneau, P.; Huc, I. *J. Am. Chem. Soc.* **2005**, *127*, 12943−12951. (e) Suginome, M.; Noguchi, H.; Murakami, M. *Chem. Lett.* **2007**, *36*, 1036−1037. (f) Kendhale, A. M.; Poniman, L.; Dong, Z.; Laxmi-Reddy, K.; Kauffmann, B.; Ferrand, Y.; Huc, I. *J. Org. Chem.* **2011**, *76*, 195−200.

(8) (a) Nelson, J. C.; Saven, J. G.; Moore, J. S.; Wolynes, P. G. *Science* **1997**, *277*, 1793−1796. For reviews, see: (b) Ray, C. R.; Moore, J. S. *Adv. Polym. Sci.* **2005**, *177*, 91−149. (c) Stone, M. T.; Heemstra, J. M.; Moore, J. S. *Acc. Chem. Res.* **2006**, *39*, 11−20. (d) Zhao, Y.; Moore, J. S. In *Foldamers: Structure, Properties, and Applications*; Hecht, S., Huc, I., Eds.; Wiley-VCH: Weinheim, 2007; Chapter 3, pp 75−108.

(9) (a) Prince, R. B.; Barnes, S. A.; Moore, J. S. *J. Am. Chem. Soc.* **2000**, *122*, 2758−2762. (b) Tanatani, A.; Mio, M. J.; Moore, J. S. *J. Am. Chem. Soc.* **2001**, *123*, 1792−1793. (c) Tanatani, A.; Hughes, T. S.; Moore, J. S. *Angew. Chem., Int. Ed.* **2002**, *41*, 325−328. (d) Stone, M. T.; Moore, J. S. *Org. Lett.* **2004**, *6*, 469−472. (e) Goto, K.; Moore, J. S. *Org. Lett.* **2005**, *7*, 1683−1686.

(10) (a) Prince, R. B.; Brunsveld, L.; Meijer, E. W.; Moore, J. S. *Angew. Chem., Int. Ed.* **2000**, *39*, 228−230. (b) Brunsveld, L.; Prince, R. B.; Meijer, E. W.; Moore, J. S. *Org. Lett.* **2000**, *2*, 1525−1528. (c) Prince, R. B.; Moore, J. S.; Brunsveld, L.; Meijer, E. W. *Chem.-Eur. J.* **2001**, *7*, 4150−4154. (d) Brunsveld, L.; Meijer, E. W.; Prince, R. B.; Moore, J. S. *J. Am. Chem. Soc.* **2001**, *123*, 7978−7984. (e) Goto, H.; Heemstra, J. M.; Hill, D. J.; Moore, J. S. *Org. Lett.* **2004**, *6*, 889−892.

(11) (a) Gin, M. S.; Yokozawa, T.; Prince, R. B.; Moore, J. S. *J. Am. Chem. Soc.* **1999**, *121*, 2643−2644. (b) Gin, M. S.; Moore, J. S. *Org. Lett.* **2000**, *2*, 135−138. (c) Hill, D. J.; Moore, J. S. *Proc. Natl. Acad. Sci. U.S.A.* **2002**, *99*, 5053−5057. (d) Stone, M. T.; Fox, J. M.; Moore, J. S. *Org. Lett.* **2004**, *6*, 3317−3320.
(12) (a) Shinohara, K.-i.; Aoki, T.; Kaneko, T.; Oikawa, E. *Polymer* **2001**, *42*, 351−355. (b) Hecht, S.; Khan, A. *Angew. Chem., Int. Ed.* **2003**, *42*, 6021−6024. (c) Ramos, A. M.; Meskers, S. C. J.; Beckers, E. H. A.; Prince, R. B.; Brunsveld, L.; Janssen, R. A. J. *J. Am. Chem. Soc.* **2004**, *126*, 9630−9644. (d) Arnt, L.; Tew, G. N. *Macromolecules* **2004**, *37*, 1283−1288. (e) Khan, A.; Kaiser, C.; Hecht, S. *Angew. Chem., Int. Ed.* **2006**, *45*, 1878−1881. (f) Khan, A.; Hecht, S. *Chem.-Eur. J.* **2006**, *12*, 4764−4774. (g) Li, C.; Guo, Y.; Lv, J.; Xu, J.; Li, Y.; Wang, S.; Liu, H.; Zhu, D. *J. Polym. Sci., Part A: Polym. Chem.* **2007**, *45*, 1403−1412. (h) Kaneko, T.; Yoshimoto, S.; Hadano, S.; Teraguchi, M.; Aoki, T. *Polyhedron* **2007**, *26*, 1825−1829. (i) Inoue, M.; Teraguchi, M.; Aoki, T.; Hadano, S.; Namikoshi, T.; Marwanta, E.; Kaneko, T. *Synth. Met.* **2009**, *159*, 854−858. (j) Sogawa, H.; Shiotsuki, M.; Matsuoka, H.; Sanda, F. *Macromolecules* **2011**, *44*, 3338−3345.
(13) (a) Inouye, M.; Waki, M.; Abe, H. *J. Am. Chem. Soc.* **2004**, *126*, 2022−2027. (b) Abe, H.; Masuda, N.; Waki, M.; Inouye, M. *J. Am. Chem. Soc.* **2005**, *127*, 16189−16196. (c) Waki, M.; Abe, H.; Inouye, M. *Chem.-Eur. J.* **2006**, *12*, 7839−7847. (d) Abe, H.; Murayama, D.; Kayamori, F.; Inouye, M. *Macromolecules* **2008**, *41*, 6903−6909. (e) Abe, H.; Machiguchi, H.; Matsumoto, S.; Inouye, M. *J. Org. Chem.* **2008**, *73*, 4650−4661.
(14) (a) Tan, C.; Pinto, M. R.; Kose, M. E.; Ghiviriga, I.; Schanze, K. S. *Adv. Mater.* **2004**, *16*, 1208−1212. (b) Zhao, X.; Schanze, K. S. *Langmuir* **2006**, *22*, 4856−4862. (c) Liu, R.; Shiotsuki, M.; Masuda, T.; Sanda, F. *Macromolecules* **2009**, *42*, 6115−6122. (d) Liu, R.; Sogawa, H.; Shiotsuki, M.; Masuda, T.; Sanda, F. *Polymer* **2010**, *51*, 2255−2263. (e) Ji, E.; Wu, D.; Schanze, K. S. *Langmuir* **2010**, *26*, 14427−14429. (f) Huang, Y.-Q.; Fan, Q.-L.; Liu, X.-F.; Fu, N.-N.; Huang, W. *Langmuir* **2010**, *26*, 19120−19128.
(15) (a) Prince, R. B.; Saven, J. G.; Wolynes, P. G.; Moore, J. S. *J. Am. Chem. Soc.* **1999**, *121*, 3114−3121. (b) Yang, W. Y.; Prince, R. B.; Sabelko, J.; Moore, J. S.; Gruebele, M. *J. Am. Chem. Soc.* **2000**, *122*, 3248−3249. (c) Lahiri, S.; Thompson, J. L.; Moore, J. S. *J. Am. Chem. Soc.* **2000**, *122*, 11315−11319.
(16) Matsuda, K.; Stone, M. T.; Moore, J. S. *J. Am. Chem. Soc.* **2002**, *124*, 11836−11837.
(17) (a) Prest, P.-J.; Prince, R. B.; Moore, J. S. *J. Am. Chem. Soc.* **1999**, *121*, 5933−5939. (b) Mio, M. J.; Prince, R. B.; Moore, J. S.; Kübel, C.; Martin, D. C. *J. Am. Chem. Soc.* **2000**, *122*, 6134−6135. (c) Kübel, C.; Mio, M. J.; Moore, J. S.; Martin, D. C. *J. Am. Chem. Soc.* **2002**, *124*, 8605−8610.
(18) Kelley, R. F.; Rybtchinski, B.; Stone, M. T.; Moore, J. S.; Wasielewski, M. R. *J. Am. Chem. Soc.* **2007**, *129*, 4114−4115.
(19) (a) Pickholz, M.; Stafström, S. *Chem. Phys.* **2001**, *270*, 245−251. (b) Elmer, S.; Pande, V. S. *J. Phys. Chem. B* **2001**, *105*, 482−485. (c) Sen, S. *J. Phys. Chem. B* **2002**, *106*, 11343−11350. (d) Lee, O.-S.; Saven, J. G. *J. Phys. Chem. B* **2004**, *108*, 11988−11994. (e) Elmer, S. P.; Pande, V. S. *J. Chem. Phys.* **2004**, *121*, 12760−12771. (f) Adisa, B.; Bruce, D. A. *J. Phys. Chem. B* **2005**, *109*, 7548−7556. (g) Adisa, B.; Bruce, D. A. *J. Phys. Chem. B* **2005**, *109*, 19952−19959. (h) Elmer, S. P.; Park, S.; Pande, V. S. *J. Chem. Phys.* **2005**, *123*, 114902. (i) Elmer, S. P.; Park, S.; Pande, V. S. *J. Chem. Phys.* **2005**, *123*, 114903. (j) Nguyen, H. H.; McAliley, J. H.; Batson, W. R.; Bruce, D. A. *Macromolecules* **2010**, *43*, 5932−5942. (k) Nguyen, H. H.; McAliley, J. H.; Bruce, D. A. *Macromolecules* **2011**, *44*, 60−67.
(20) Tanaka, H.; Kawai, T. *Nat. Nanotechnol.* **2009**, *4*, 518−522.
(21) (a) Sakurai, S.-i.; Okoshi, K.; Kumaki, J.; Yashima, E. *Angew. Chem., Int. Ed.* **2006**, *45*, 1245−1248. (b) Sakurai, S.-i.; Okoshi, K.; Kumaki, J.; Yashima, E. *J. Am. Chem. Soc.* **2006**, *128*, 5650−5651. (c) Sakurai, S.-i.; Ohsawa, S.; Nagai, K.; Okoshi, K.; Kumaki, J.; Yashima, E. *Angew. Chem., Int. Ed.* **2007**, *46*, 7605−7608. (d) Louzao, I.; Seco, J. M.; Quiñoá, E.; Riguera, R. *Angew. Chem., Int. Ed.* **2010**, *49*, 1430−1433. (e) Freire, F.; Seco, J. M.; Quiñoá, E.; Riguera, R. *Angew. Chem., Int. Ed.* **2011**, *50*, 11692−11696. (f) Ohsawa, S.; Sakurai, S.-i.; Nagai, K.; Banno, M.; Maeda, K.; Kumaki, J.; Yashima, E. *J. Am. Chem. Soc.* **2011**, *133*, 108−114. (g) Ohsawa, S.; Sakurai, S.-i.; Nagai, K.; Maeda, K.; Kumaki, J.; Yashima, E. *Polym. J.* **2011**, 1−9. For reviews, see refs 1m, 1n, 1r, and 4, and (h) Kumaki, J.; Sakurai, S.-i.; Yashima, E. *Chem. Soc. Rev.* **2009**, *38*, 737−746.
(22) (a) Kajitani, T.; Okoshi, K.; Sakurai, S.-i.; Kumaki, J.; Yashima, E. *J. Am. Chem. Soc.* **2006**, *128*, 708−709. (b) Onouchi, H.; Okoshi, K.; Kajitani, T.; Sakurai, S.-i.; Nagai, K.; Kumaki, J.; Onitsuka, K.; Yashima, E. *J. Am. Chem. Soc.* **2008**, *130*, 229−236. (c) Wu, Z.-Q.; Nagai, K.; Banno, M.; Okoshi, K.; Onitsuka, K.; Yashima, E. *J. Am. Chem. Soc.* **2009**, *131*, 6708−6718. (d) Banno, M.; Wu, Z.-Q.; Nagai, K.; Sakurai, S.-i.; Okoshi, K.; Yashima, E. *Macromolecules* **2010**, *43*, 6553−6561. (e) Kumaki, J.; Kajitani, T.; Nagai, K.; Okoshi, K.; Yashima, E. *J. Am. Chem. Soc.* **2010**, *132*, 5604−5606. (f) Miyabe, T.; Iida, H.; Banno, M.; Yamaguchi, T.; Yashima, E. *Macromolecules* **2011**, *44*, 8687−8692.
(23) Kumaki, J.; Kawauchi, T.; Okoshi, K.; Kusanagi, H.; Yashima, E. *Angew. Chem., Int. Ed.* **2007**, *46*, 5348−5351.
(24) Maeda, T.; Furusho, Y.; Sakurai, S.-i.; Kumaki, J.; Okoshi, K.; Yashima, E. *J. Am. Chem. Soc.* **2008**, *130*, 7938−7945.
(25) Khan, A.; Hecht, S. *Chem. Commun.* **2004**, 300−301.
(26) For oligo(*m*-phenylene ethynylene) derivatives whose helical conformations are stabilized by intramolecular hydrogen bonds, see: (a) Cary, J. M.; Moore, J. S. *Org. Lett.* **2002**, *4*, 4663−4666. (b) Yang, X.; Brown, A. L.; Furukawa, M.; Li, S.; Gardinier, W. E.; Bukowski, E. J.; Bright, F. V.; Zheng, C.; Zeng, X. C.; Gong, B. *Chem. Commun.* **2003**, 56−57. The molecular dynamics simulation studies also supported such intramolecular hydrogen bonds formed between the amide groups, resulting in a stable helical conformation of an oligo(*m*-phenylene ethynylene) bearing amide pendants in chloroform. See refs 19j and 19k. For other helical polymers and foldamers whose helical structures are stabilized by intramolecular hydrogen bonds, see refs 2d, 2f−i, 12j, 14c, and 14d. For polyisocyanides: (c) Cornelissen, J. J. L. M.; Donners, J. J. J. M.; de Gelder, R.; Graswinckel, W. S.; Metselaar, G. A.; Rowan, A. E.; Sommerdijk, N. A. J. M.; Nolte, R. J. M. *Science* **2001**, *293*, 676−680. (d) de Witte, P. A. J.; Hernando, J.; Neuteboom, E. E.; van Dijk, E. M. H. P.; Meskers, S. C. J.; Janssen, R. A. J.; van Hulst, N. F.; Nolte, R. J. M.; García-Parajó, M. F.; Rowan, A. E. *J. Phys. Chem. B* **2006**, *110*, 7803−7812. (e) Hase, Y.; Mitsutsuji, Y.; Ishikawa, M.; Maeda, K.; Okoshi, K.; Yashima, E. *Chem.-Asian J.* **2007**, *2*, 755−763. (f) Okoshi, K.; Nagai, K.; Kajitani, T.; Sakurai, S.-i.; Yashima, E. *Macromolecules* **2008**, *41*, 7752−7754. For poly(*N*-propargylamide)s: (g) Nomura, R.; Tabei, J.; Masuda, T. *J. Am. Chem. Soc.* **2001**, *123*, 8430−8431. (h) Nomura, R.; Tabei, J.; Masuda, T. *Macromolecules* **2002**, *35*, 2955−2961. (i) Gao, G.; Sanda, F.; Masuda, T. *Macromolecules* **2003**, *36*, 3932−3937. (j) Tabei, J.; Shiotsuki, M.; Sanda, F.; Masuda, T. *Macromolecules* **2005**, *38*, 5860−5867. For poly(*N*-propargylcarbamate)s: (k) Nomura, R.; Nishiura, S.; Tabei, J.; Sanda, F.; Masuda, T. *Macromolecules* **2003**, *36*, 5076−5080. For poly(*N*-propargylsulfamide)s: (l) Deng, J.; Tabei, J.; Shiotsuki, M.; Sanda, F.; Masuda, T. *Macromolecules* **2004**, *37*, 5538−5543. For poly(propargyl ester)s: (m) Sanda, F.; Araki, H.; Masuda, T. *Macromolecules* **2005**, *38*, 10605−10608. For poly(*N*-propargylphosphonamidate)s: (n) Yue, D.; Fujii, T.; Terada, K.; Tabei, J.; Shiotsuki, M.; Sanda, F.; Masuda, T. *Macromol. Rapid Commun.* **2006**, *27*, 1460−1464. For poly(*N*-propargylurea)s: (o) Deng, J.; Luo, X.; Zhao, W.; Yang, W. *J. Polym. Sci., Part A: Polym. Chem.* **2008**, *46*, 4112−4121. For poly(*N*-butynylamide)s: (p) Suzuki, Y.; Tabei, J.; Shiotsuki, M.; Inai, Y.; Sanda, F.; Masuda, T. *Macromolecules* **2008**, *41*, 1086−1093. For poly(1-methylpropargyl-*N*-alkylcarbamate)s: (q) Shirakawa, Y.; Suzuki, Y.; Terada, K.; Shiotsuki, M.; Masuda, T.; Sanda, F. *Macromolecules* **2010**, *43*, 5575−5581. For poly(phenylacetylene)s: (r) Li, B. S.; Cheuk, K. K. L.; Salhi, F.; Lam, J. W. Y.; Cha, J. A. K.; Xiao, X.; Bai, C.; Tang, B. Z. *Nano Lett.* **2001**, *1*, 323−328. (s) Aoki, T.; Kaneko, T.; Maruyama, N.; Sumi, A.; Takahashi, M.; Sato, T.; Teraguchi, M. *J. Am. Chem. Soc.* **2003**, *125*, 6346−6347. (t) Okoshi, K.; Sakajiri, K.; Kumaki, J.; Yashima, E. *Macromolecules* **2005**, *38*, 4061−4064. (u) Terada, K.; Masuda, T.; Sanda, F. *Macromolecules* **2009**, *42*, 913−920.

(27) Although weak meridional reflections at 4.00, 3.27, and 2.86 Å were also observed for (*S*)-**PPEa**, we could not characterize these reflections, which may be related to the electron densities along with the main-chain axis.

(28) When the sample was exposed to organic solvent vapors according to a previously reported method,[21,22,24] almost similar AFM images were obtained, indicating that organic solvent vapors may not be essential for obtaining 2D assembled helix-bundles at least for **PPEa**.

(29) Casting a more dilute solution (0.01 mg/mL) of (*S*)-**PPEa** on HOPG produced the isolated monolayers with an average height of 0.4 nm (first layer, Figure S4), which was much less than the molecular diameter of a helically folded **PPEa** model (3.2 nm). Further deposition of the same dilute solution on the monolayers on HOPG resulted in the formation of the 2D helix-bundled (*S*)-**PPEa** assemblies (second layer) whose AFM images were almost identical to those shown in Figure 5A.

(30) When (*S*)-**PPEa** has such a right-handed helical array of the pendants, the main-chain has a 5.7 units per turn right-handed helical structure.

(31) For review on the synthesis of cyclic polymers, see: (a) Laurent, B. A.; Grayson, S. M. *Chem. Soc. Rev.* **2009**, *38*, 2202−2213. For recent examples of AFM observations of cyclic polymers, see: (b) Kawaguchi, D.; Nishu, T.; Takano, A.; Matsushita, Y. *Polym. J.* **2007**, *39*, 271−275. (c) Schappacher, M.; Deffieux, A. *Science* **2008**, *319*, 1512−1515. (d) Schappacher, M.; Deffieux, A. *J. Am. Chem. Soc.* **2008**, *130*, 14684−14689. (e) Schappacher, M.; Deffieux, A. *Angew. Chem., Int. Ed.* **2009**, *48*, 5930−5933. (f) Boydston, A. J.; Holcombe, T. W.; Unruh, D. A.; Fréchet, J. M. J.; Grubbs, R. H. *J. Am. Chem. Soc.* **2009**, *131*, 5388−5389. (g) Xia, Y.; Boydston, A. J.; Grubbs, R. H. *Angew. Chem., Int. Ed.* **2011**, *50*, 5882−5885. (h) Lahasky, S. H.; Serem, W. K.; Guo, L.; Garno, J. C.; Zhang, D. *Macromolecules* **2011**, *44*, 9063−9074. (i) Zhang, K.; Lackey, M. A.; Wu, Y.; Tew, G. N. *J. Am. Chem. Soc.* **2011**, *133*, 6906−6909.

(32) For related Vernier-templating, see: O'Sullivan, M. C.; Sprafke, J. K.; Kondratuk, D. V.; Rinfray, C.; Claridge, T. D. W.; Saywell, A.; Blunt, M. O.; O'Shea, J. N.; Beton, P. H.; Malfois, M.; Anderson, H. L. *Nature* **2011**, *469*, 72−75.